

## Rearrangement, Nucleophilic Substitution, and Halogen Switch Reactions of Alkyl Halides over NaY Zeolite: Formation of the Bicyclobutonium Cation Inside the Zeolite Cavity

Marcelo Franco,<sup>†</sup> Nilton Rosenbach, Jr.,<sup>†</sup> Glaucio B. Ferreira,<sup>†</sup> Antônio C. O. Guerra,<sup>‡</sup> W. Bruce Kover,<sup>†</sup> Cássia C. Turci,<sup>†</sup> and Claudio J. A. Mota\*<sup>†</sup>

Universidade Federal do Rio de Janeiro, Instituto de Química, Av Athos da Silveira Ramos 149, CT Bloco A, Cidade Universitária 21941-909, Rio de Janeiro, Brazil and Centro Federal de Educação Tecnológica Celso Suckow da Fonseca, Rio de Janeiro, 20271-110, Brazil

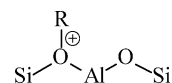
Received June 27, 2007; E-mail: cmota@iq.ufrj.br

**Abstract:** Rearrangement and nucleophilic substitution of cyclopropylcarbinyl bromide over NaY and NaY impregnated with NaCl was observed at room temperature. The first-order kinetics are consistent with ionization to the bicyclobutonium cation, followed by internal return of the bromide anion or nucleophilic attack by impregnated NaCl to form cyclopropylcarbinyl, cyclobutyl, and allylcarbinyl chlorides. The product distribution analysis revealed that neither a purely kinetic distribution, similar to what is found in solution, nor the thermodynamic ratio, which favors the allylcarbinyl halide, was observed. Calculations showed that bicyclobutonium and cyclopropylcarbinyl carbocations are minimal over the zeolite structure, and stabilized by hydrogen bonding with the framework structure. A new process of nucleophilic substitution is reported, namely halogen switch, involving alkyl chlorides and bromides of different structures. The reaction occurs inside the zeolite pores, due to the confinement effects and is an additional proof of carbocation formation on zeolites. The results support the idea that zeolites act as solid solvents, permitting ionization and solvation of ionic species.

### Introduction

Zeolites are aluminosilicates with three-dimensional framework structures forming channels and cages with molecular dimensions.<sup>1</sup> They are widely used as catalysts in the petrochemical industry, in cracking, isomerization, and alkylation processes.<sup>2</sup> Due to the confined space inside the porous structure, the shape-selectivity property of zeolites has been explored as a nanoreactor system, both in traditional organic chemistry<sup>3</sup> as well as in photochemical reactions.<sup>4</sup> By analogy with superacid media,<sup>5</sup> carbocations are believed to be key intermediates in zeolite catalyzed hydrocarbon transformations, where the zeolites act as Bronsted acids, transferring a proton to the hydrocarbon. However, simple carbocationic species are seldom observed on the zeolite surface as persistent intermediates. Indeed, only some conjugated cyclic carbocations were observed as long-lived species, but covalent intermediates, namely alkoxides<sup>6</sup> (Chart 1), are usually thermodynamically more stable than simple alkyl carbocation,<sup>7</sup> and observed as persistent

**Chart 1.** Pictorial Representation of the Alkoxide on the Zeolite Surface



intermediates on the zeolite surface. Some studies suggest that alkoxides should be the real intermediates involved in hydrocarbon reactions over zeolite, whereas carbocations are just transition states on these reactions.<sup>8</sup> Equilibrium between the alkoxides and the carbocations, although suggested in some cases, has never been experimentally or theoretically proven, but recent calculations indicated that the *tert*-butyl carbenium ion might be an intermediate on some specific zeolite structures, being more stable than the respective alkoxide, depending on the temperature employed.<sup>9</sup>

Cation-exchanged zeolites have been used to photochemically generate radicals,<sup>10</sup> conjugated carbocations,<sup>11</sup> and carbenes<sup>12</sup> inside the zeolite cage. The electron-accepting ability of the compensating cation influences the reactivity of these species

<sup>†</sup> Universidade Federal do Rio de Janeiro, Instituto de Química.

<sup>‡</sup> Centro Federal de Educação Tecnológica Celso Suckow da Fonseca.

(1) Breck, D. W. *Zeolite Molecular Sieves: Structure, Chemistry and Use*; Wiley: New York, 1974.

(2) Corma, A. *Chem. Rev.* **1995**, *95*, 559.

(3) Smith, K. *Bull. Soc. Chim. Fr.* **1989**, 272.

(4) Turro, N. J. *Acc. Chem. Res.* **2000**, *33*, 637.

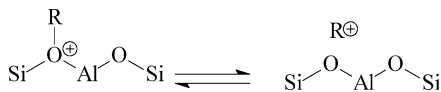
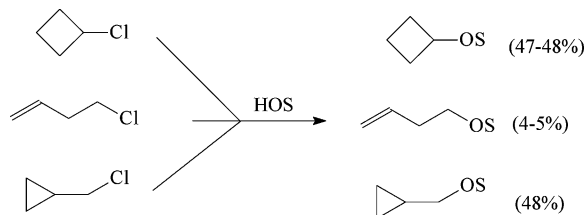
(5) Olah, G. A.; Prakash, G. K. S.; Sommer, J. *Superacids*; Wiley: New York, 1995.

(6) Haw, J. F.; Nicholas, J. B.; Xu, T.; Beck, L. W.; Ferguson, D. B. *Acc. Chem. Res.* **1996**, *29*, 259.

(7) (a) Aronson, M. T.; Gorte, R. J.; Farneth, W. E.; White, D. *J. Am. Chem. Soc.* **1989**, *111*, 840. (b) Haw, J. F.; Richardson, B. R.; Oshiro, I. S.; Lazo, N. D.; Speed, J. A. *J. Am. Chem. Soc.* **1989**, *111*, 2052.

(8) (a) Kazansky, V. B. *Acc. Chem. Res.* **1991**, *24*, 379. (b) Viruela-Martin, P.; Zicovich-Wilson, C. M.; Corma, A. *J. Phys. Chem.* **1993**, *97*, 13713. (c) Kazansky, V. B.; Frash, M. V.; van Santen, R. A. *Appl. Catal. A* **1996**, *146*, 225.

(9) (a) Boronat, M.; Viruela, P. M.; Corma, A. *J. Am. Chem. Soc.* **2004**, *126*, 3300. (b) Tuma, C.; Sauer, J. *Angew. Chem., Int. Ed.* **2005**, *44*, 4769.

**Scheme 1.** Possible Equilibrium between the Alkoxide and the Carbocation on the Zeolite Surface**Scheme 2.** Product Distribution from Solvolysis of Cyclopropylcarbinyl, Cyclobutyl, and Allylcarbinyl Chlorides

inside the zeolite, which may also be related with the polarity of the medium. We have been using cation-exchanged zeolites as alkylating catalysts<sup>13</sup> and to study the formation and reactivity of the alkoxides.<sup>14</sup> The main advantage over protonic zeolites is that secondary side reactions, such as oligomerization, are reduced. In these studies, the metal cation acts as a Lewis acid site, coordinating with an alkylhalide to form a metal-halide species and an alkoxide bonded to the zeolite structure. However, it was neither possible to observe the carbocations as discrete intermediates, nor to show the equilibrium between the carbocation and the alkoxide (Scheme 1) in those studies.

The rearrangement of the cyclopropylcarbinyl chloride in solution is well documented in the literature.<sup>15</sup> In polar solvents, three products, arisen from the nucleophilic substitution of the solvent to the chloride, are usually detected. They are formed via nucleophilic substitution of the chloride by the solvent. This chemistry can be explained by the formation of a  $C_4H_7^+$  cation, which acts as a tridentate ion, generating the three products shown in Scheme 2.

The  $^{13}C$  NMR spectrum of the  $C_4H_7^+$  cation in superacidic solution shows a single peak for the three methylene carbon atoms.<sup>16</sup> This equivalence can be explained by a nonclassical single symmetric (3-fold) structure. However, studies on the solvolysis of labeled cyclopropylcarbinyl derivatives suggest a degenerate equilibrium among carbocations with lower symmetry, instead of the 3-fold symmetrical species.<sup>17</sup> A small

temperature dependence of the  $^{13}C$  chemical shifts indicated the presence of two carbocations, one of them in small amounts but still in equilibrium with the major species. This conclusion was supported by isotope perturbation experiments.<sup>18</sup> The classical cyclopropylcarbinyl cation and the nonclassical bicyclobutonium cation were considered as the most likely species participating in this equilibrium.

Alternatively, many theoretical methods have been employed to elucidate the potential energy surface of the  $C_4H_7^+$  in gas phase<sup>19</sup> and in solution.<sup>20</sup> High-level ab initio calculations suggest that, in the gas phase, there are three  $C_4H_7^+$  structures as minima on the potential energy surface. These calculations pointed to the bicyclobutonium and cyclopropylcarbinyl cations as the most stable structures.

In this work, we report experimental and theoretical results on the rearrangement and nucleophilic substitution of cyclopropylcarbinyl and cyclobutyl halides over NaY zeolite, aiming at demonstrating the formation of  $C_4H_7^+$  cations as discrete intermediates inside the zeolite cavity. A new process of nucleophilic substitution, which we have named halogen switch, was encountered in these studies. This reaction supports the hypothesis that carbocations are intermediates inside the zeolite cavity and might be in equilibrium with alkoxides. This reaction also gives additional information of the ability of the zeolite cage to confine ionic species.

## Experimental Section

The reactions were studied on a NaY zeolite (Si/Al = 2.6 and surface area of  $704 \text{ m}^2 \text{ g}^{-1}$ ) and on NaY impregnated with NaBr or NaCl. These latter samples were prepared by soaking the NaY zeolite with an aqueous solution of NaBr or NaCl, followed by water evaporation in a rotary evaporator. The impregnation was performed to yield about 10 wt % of chloride or bromide ions into the zeolite (in dry base). In a typical procedure, 4.5 g (dry base) of the NaY zeolite was treated with 75 mg of sodium chloride dissolved in 100 mL of deionized water.

The reactions were carried out in a glass unit with a straight reactor (fixed bed) at room temperature and atmospheric pressure. About 200 mg of the zeolite was initially pretreated for 30 min at  $300 \text{ }^\circ\text{C}$  ( $2.5 \text{ }^\circ\text{C min}^{-1}$ ), under  $N_2$  atmosphere ( $40 \text{ mL min}^{-1}$ ). The reactor was cooled to room temperature and 0.5 mL of the alkylhalide was injected in the  $N_2$  flow, with the use of a syringe. The products were collected at the reactor outlet, using a trap immersed in ice bath. The products were separated by a gas chromatograph coupled to a mass quadrupole spectrometer, using electron impact ionization (70 eV). For the halogen switch, the experimental procedure was similar, except for the introduction of an equimolar mixture of an alkyl bromide and an alkyl chloride of different structures.

A batch procedure was used for the kinetic experiments. About 500 mg of the zeolite was initially pretreated at  $300 \text{ }^\circ\text{C}$  for 30 min in a round-bottom flask. After cooling to room temperature a solution containing 0.1 mmol of the alkylhalide in *n*-pentane, together with a known amount of *n*-heptane used as internal standard, was introduced into the flask. The kinetics, at  $25 \text{ }^\circ\text{C}$ , were followed, withdrawing samples of the liquid phase for analysis at specific time intervals.

To have some insight of the dispersion of the NaCl and NaBr into the zeolite channels, we carried out a preliminary analysis using the soft X-ray Spectroscopy (SXS) beam line at the National Laboratory

- (10) (a) Cozens, F. L.; Ortiz, W.; Schepp, N. P. *J. Am. Chem. Soc.* **1998**, *120*, 13543. (b) Cozens, F. L.; Cano, M. L.; Garcia, H.; Schepp, N. P. *J. Am. Chem. Soc.* **1998**, *120*, 5667.
- (11) (a) Cozens, F. L.; O'Neil, M. A.; Schepp, N. P. *J. Am. Chem. Soc.* **1997**, *119*, 7583. (b) O'Neil, M. A.; Cozens, F. L.; Schepp, N. P. *Tetrahedron* **2000**, *56*, 6969. (c) Koodanjeri, S.; Ramamurthy, V. *Tetrahedron Lett.* **2003**, *44*, 1615.
- (12) (a) Moya-Barrios, R.; Cozens, F. L. *Org. Lett.* **2004**, *6*, 881. (b) Moya-Barrios, R.; Cozens, F. L. *J. Am. Chem. Soc.* **2006**, *128*, 14836.
- (13) (a) Bidart, A. M. F.; Borges, A. P. S.; Nogueira, L.; Lachter, E. R.; Mota, C. J. A. *Catal. Lett.* **2001**, *75*, 155. (b) Rosenbach, N., Jr.; Mota, C. J. A. *J. Braz. Chem. Soc.* **2005**, *16*, 691. (c) Noronha, L. A.; Mota, C. J. A. *Catal. Today* **2005**, *101*, 9. (d) Bidart, A. M. F.; Borges, A. P. S.; Chagas, H. C.; Nogueira, L.; Lachter, E. R.; Mota, C. J. A. *J. Braz. Chem. Soc.* **2006**, *17*, 758.
- (14) (a) Corrêa, R. J.; Mota, C. J. A. *Phys. Chem. Chem. Phys.* **2002**, *4*, 4268. (b) Corrêa, R. J.; Mota, C. J. A. *Appl. Catal. A* **2003**, *255*, 255. (c) Rosenbach, N., Jr.; Mota, C. J. A. *J. Molec. Struct. (Theochem)* **2005**, *731*, 157.
- (15) (a) Roberts, J. D.; Mazur, R. H. *J. Am. Chem. Soc.* **1951**, *73*, 2509. (b) Mazur, R. H.; White, W. N.; Semenov, D. A.; Lee, C. C.; Silver, M. S.; Roberts, J. D. *J. Am. Chem. Soc.* **1958**, *81*, 4390. (c) Siehl, H. U. In *The Chemistry of Cyclobutanes*; Rappoport, Z., Liebman, J. F., Eds.; Wiley: New York, 2005; p 512.
- (16) Olah, G. A.; Kelly, D. P.; Jeuell, C. J.; Porter, R. D. *J. Am. Chem. Soc.* **1970**, *93*, 2544.
- (17) Starat, J. S.; Roberts, J. D.; Prakash, G. K. S.; Donovan, D. J.; Olah, G. A. *J. Am. Chem. Soc.* **1978**, *100*, 8016.

- (18) (a) Saunders, M.; Siehl, H. U. *J. Am. Chem. Soc.* **1988**, *110*, 6868. (b) Koch, W.; Liu, B.; Defrees, D. J. *J. Am. Chem. Soc.* **1988**, *110*, 7225.
- (19) (a) Saunders, M.; Laidig, M.; Wiberg, K. E.; Schleyer, P. v. R. *J. Am. Chem. Soc.* **1988**, *110*, 7652.
- (20) Casanova, J.; Kent, D. R., IV; Goddard, W. A., III; Roberts, J. D. *Proc. Nat. Acad. Sci.* **2003**, *100*, 15.

of Synchrotron Light (LNLS), in Campinas, Brazil. The X-ray photoelectron spectra (XPS) of the parent NaY and NaY impregnated with NaCl and NaBr have been measured at the Si(1s), Al(1s), Na(1s), O(1s), Cl(1s and 2p), and Br(1s and 2p) edges. Before the acquisitions, the zeolites were kept overnight at 150 °C to desorb water. The samples were introduced in the main chamber as a solid using carbon sticky tape. The work pressure was maintained at  $2 \times 10^{-8}$  mBar.

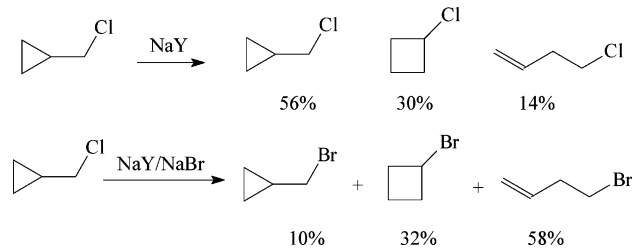
### Computational Methods

The theoretical studies were carried out employing the ONIOM scheme developed by Morokuma and collaborators.<sup>21</sup> This approach can be of great utility because it allows the study of large molecular systems, and thus, of a particular zeolite structure. In this work, we used a T<sub>48</sub> model (T = Si, Al) representing the pore aperture of the zeolite Y. The crystalline structure of the zeolite Y is formed by association of Al and Si tetrahedrons linked by oxygen atoms. The free valences of border aluminum and silicon atoms were saturated with hydrogen atoms, to avoid dangling bonds. The calculations were performed using the ONIOM method available in GAUSSIAN 98 package.<sup>22</sup> The molecular system was divided into two layers. The atoms of the active site of the zeolite Y and the organic moiety (high layer) were treated at the B3LYP/6-31G(d,p), MP2/6-31G(d,p) and PBE1PBE/6-31G(d,p) levels, whereas the other atoms (low layer) were treated by the semiempirical MNDO method. We have calculated the bicyclobutonium and cyclopropylcarbiny carbocations inside the zeolite cage. The geometry of all species were fully optimized, and characterized as minima on the potential energy surface by the absence of imaginary frequencies, after vibrational analysis of the optimized geometries. Zero-point energies (ZPE) and thermal correction were calculated at the same level of theory, except for the calculations at MP2/6-31G(d,p), in which it was used the corrections computed at PBE1PBE/6-31G(d,p). The enthalpy differences refer to 298.15K and 1 atm.

### Results and Discussions

**Rearrangement and Nucleophilic Substitution (Flow Conditions).** When a gaseous flow of cyclopropylcarbiny chloride is passed over NaY zeolite at room temperature, we were able to observe cyclobutyl chloride and allylcarbiny chloride, together with unreacted substrate in the effluent. Using NaY zeolite impregnated with NaBr, besides the three alkylchlorides we observed formation of cyclopropylcarbiny bromide, cyclobutyl bromide, and allylcarbiny bromide (Scheme 3). These results are consistent with ionization of the cyclopropylcarbiny chloride on NaY zeolite to form the C<sub>4</sub>H<sub>7</sub><sup>+</sup> cation. Attack of the chloride ion (internal return) occurs at the three electrophilic positions of the carbocation, giving the rearranged alkyl chlorides. This hypothesis was supported by the results with the impregnation of NaBr on the NaY zeolite. The observation of the three alkylbromides is consistent with a mechanism involving ionization of the cyclopropylcarbiny chloride to the bicyclobutonium cation, followed by nucleophilic attack of the

**Scheme 3.** Product Distribution for the Reaction of Cyclopropylcarbiny Chloride over NaY and NaY Impregnated with NaBr at 25 °C<sup>a</sup>



<sup>a</sup> For the latter reaction, only the alkyl bromide distribution is shown, but the alkyl chlorides were also observed experimentally.

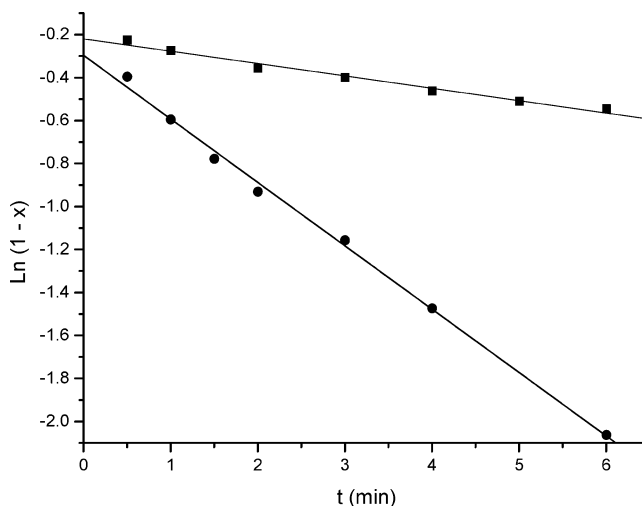


**Figure 1.** Kinetics of the cyclopropylcarbiny bromide (●;  $r^2 = 0.973$ ) and cyclopropylcarbiny chloride (■;  $r^2 = 0.958$ ) rearrangement over NaY zeolite at 25 °C (x stands for conversion).

bromide ions located inside the zeolite cages. Recently, the same kind of rearrangement was observed<sup>23</sup> on oxygen-covered Mo surfaces, proving the intermediacy of carbocations on metal surfaces.

An interesting situation arises from considerations of the product distribution from ionization of cyclopropylcarbiny chloride over NaY impregnated with NaBr. Contrary to what is found in solution, where the cyclic products are preferred, inside the zeolite pores the thermodynamically more stable allylcarbiny bromide predominates. Variation of the carrier gas (N<sub>2</sub>) flow rate did not significantly affect the alkyl bromide distribution, indicating that the contact time has little influence in the selectivity. It is possible that the alkyl bromides undergo successive ionization before escaping the pore network, favoring a distribution closer to the thermodynamic one.

**Kinetic Analysis (Batch Reactions).** Figure 1 shows the kinetics of cyclopropylcarbiny halides (chloride and bromide) rearrangement over NaY zeolite at 25 °C, and Figure 2 the kinetics of the cyclobutyl bromide. As expected, the bromide is more reactive than the respective chloride, whereas the cyclopropylcarbiny structure reacts faster than the cyclobutyl one. Table 1 reports the observed rates for the different systems studied. One can see that over NaY zeolite cyclopropylcarbiny bromide (entry 1) reacts about five times faster than cyclobutyl bromide (entry 9) and three times faster than cyclopropylcarbiny

(21) Dapprich, S.; Komáromi, I.; Byun, K. S.; Morokuma, K.; Frisch, M. J. *J. Molec. Struct. (Theochem)* **1999**, *1*, 461.

(22) Frisch, M. J.; Trucks, G. W.; Schlegel, H. B.; Scuseria, G. E.; Robb, M. A.; Cheeseman, J. R.; Zakrzewski, V. G.; Montgomery, J. A., Jr.; Stratmann, R. E.; Burant, J. C.; Dapprich, S.; Millam, J. M.; Daniels, A. D.; Kudin, K. N.; Strain, M. C.; Farkas, O.; Tomasi, J.; Barone, V.; Cossi, M.; Cammi, R.; Mennucci, B.; Pomelli, C.; Adamo, C.; Clifford, S.; Ochterski, J.; Petersson, G. A.; Ayala, P. Y.; Cui, Q.; Morokuma, K.; Malick, D. K.; Rabuck, A. D.; Raghavachari, K.; Foresman, J. B.; Cioslowski, J.; Ortiz, J. V.; Stefanov, B. B.; Liu, G.; Liashenko, A.; Piskorz, P.; Komaromi, I.; Gomperts, R.; Martin, R. L.; Fox, D. J.; Keith, T.; Al-Laham, M. A.; Peng, C. Y.; Nanayakkara, A.; Gonzalez, C.; Challacombe, M.; Gill, P. M. W.; Johnson, B. G.; Chen, W.; Wong, M. W.; Andres, J. L.; Head-Gordon, M.; Replogle, E. S.; Pople, J. A. *Gaussian 98*, revision C.3; Gaussian, Inc.: Pittsburgh, PA, 1998.

(23) Wiedemann, S. H.; Kang, D. H.; Bergman, R. G.; Friend, C. M. *J. Am. Chem. Soc.* **2007**, *129*, 4666.

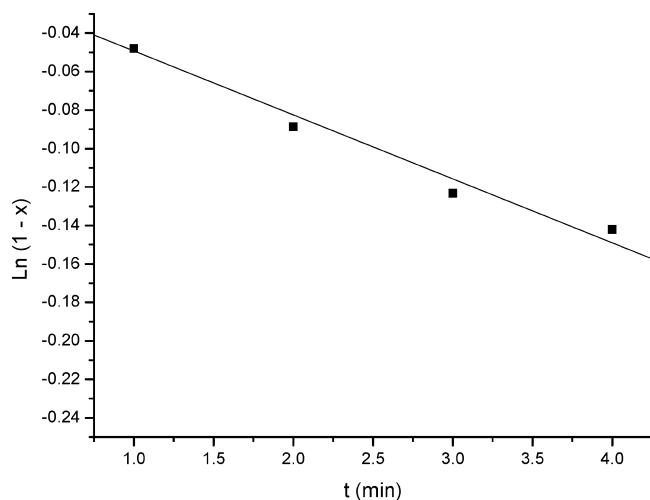


**Figure 2.** Kinetics of the cyclobutyl bromide rearrangement over NaY zeolite at 25 °C ( $r^2 = 0.968$ ).

**Table 1.** Rates of Cyclopropylcarbinyl and Cyclobutyl Halides over Zeolite NaY and Other Lewis Acid Catalysts, at 25 °C

| Entry | System   | k (min <sup>-1</sup> ) |
|-------|--|------------------------|
| 1     | $\xrightarrow{\text{NaY}}$                     | 0.159                  |
| 2     | $\xrightarrow[\text{NaCl (10\%)}]{\text{NaY}}$ | 0.142                  |
| 3     | $\xrightarrow{\text{NaY}}$                     | 0.060                  |
| 4     | $\xrightarrow[\text{NaBr (1\%)}]{\text{NaY}}$  | 0.058                  |
| 5     | $\xrightarrow[\text{NaBr (10\%)}]{\text{NaY}}$ | 0.055                  |
| 6     | $\xrightarrow{\text{ZnCl}_2}$                  | 0.007 <sup>a</sup>     |
| 7     | $\xrightarrow{\text{FeCl}_3}$                  | 0.512 <sup>a</sup>     |
| 8     | $\xrightarrow{\text{Al}_2\text{O}_3}$          | 0.0001 <sup>a</sup>    |
| 9     | $\xrightarrow{\text{NaY}}$                     | 0.033                  |
| 10    | $\xrightarrow[\text{NaCl (10\%)}]{\text{NaY}}$ | 0.022                  |

<sup>a</sup> Using the same equivalent of metal atoms of the NaY experiments.

chloride (entry 3). The impregnation of the zeolite with NaCl or NaBr (entries 2 and 4) does not significantly alter the rates, supporting a mechanism involving ionization of the alkyl halide as the rate-determining step. Even with a 10-fold excess of impregnated bromide ions (entries 4 and 5) over NaY, the reaction rate was practically the same, giving strong arguments for a first-order reaction, independent of the NaBr concentration. A control experiment with the cyclopropylcarbinyl or cyclobutyl halide with the correspondent sodium halide in *n*-pentane did not show any significant rearrangement of the hydrocarbon structure, indicating that no ionization occurs in the apolar *n*-pentane medium, in absence of zeolite.

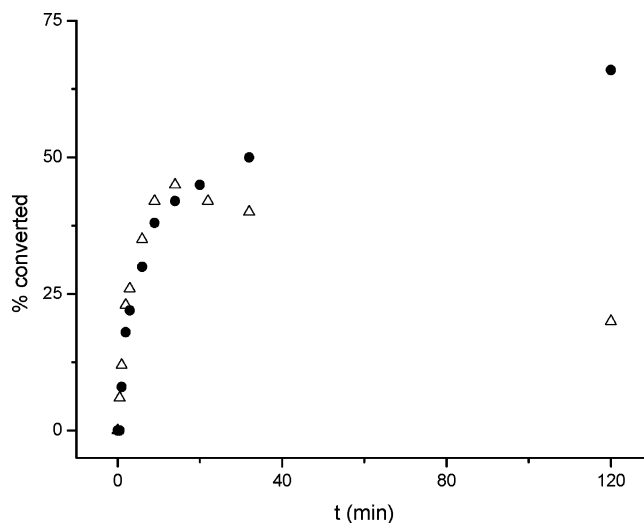


**Figure 3.** Product formation in the rearrangement of cyclopropylcarbinyl bromide over NaY zeolite at 25 °C; (●) allylcarbinyl bromide; and (Δ) cyclobutyl bromide.

Table 1 also shows the kinetics of cyclopropylcarbinyl chloride catalyzed by traditional Lewis acids, such as FeCl<sub>3</sub>, ZnCl<sub>2</sub>, and Al<sub>2</sub>O<sub>3</sub> (entries 6 to 8). Only ferric chloride was a more efficient catalyst for the rearrangement than NaY zeolite. Zinc chloride reacted about 10 fold slower than NaY zeolite, whereas Al<sub>2</sub>O<sub>3</sub> was less active to catalyze the rearrangement by a factor of 100.

Figure 3 shows the product distribution analysis for the rearrangement of cyclopropylcarbinyl bromide over NaY zeolite as a function of time. One can see that while the reactant is almost consumed in the first 20 min of reaction, cyclobutyl and allylcarbinyl bromides are formed in approximately the same amount (about 50% each). However, after 20 min, the concentration of the cyclobutyl bromide decreases, while the concentration of the allylcarbinyl continues to rise. This is consistent with the higher thermodynamic stability of the allylcarbinyl halide, which is being accumulated in the reaction medium as the reaction time increases. The cyclobutyl bromide rearranges further, and after 20 min, its consumption rate is higher than its formation rate. A similar pattern was observed in the reaction with FeCl<sub>3</sub>.

Figure 4 shows the distribution of the alkyl chlorides formed upon the ionization of cyclopropylcarbinyl bromide over NaY impregnated with 10% NaCl. At the beginning of the reaction, the cyclopropylcarbinyl chloride is formed in higher yield than the cyclobutyl and allylcarbinyl chlorides. Nevertheless, after 10 min, its concentration starts going down, while the concentration of the cyclobutyl and allylcarbinyl chlorides continues to increase. This is consistent with the higher reactivity of the cyclopropylcarbinyl system, which starts to decompose as its concentration and reaction time increase. Alternatively, the distribution of the allylcarbinyl chloride is always higher than the kinetic distribution found in solution, even at short reaction times. The concentration of cyclopropylcarbinyl chloride decreases with time, going to 0 after 120 min, while the distribution of the other two chlorides increases. The distribution of cyclobutyl chloride and allylcarbinyl chloride is slightly affected after 60 min of reaction time. It is not completely clear why a distribution that is neither thermodynamic nor kinetic is observed within the pore structure of zeolite Y. In the FeCl<sub>3</sub>-catalyzed

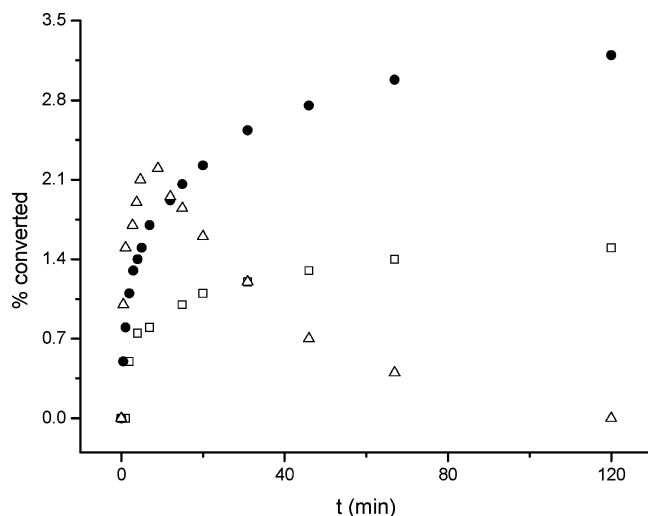


**Figure 4.** Alkylchlorides formation in the rearrangement of cyclopropylcarbinyl bromide over NaY zeolite impregnated with NaCl at 25 °C; ( $\Delta$ ) cyclopropylcarbinyl chloride; ( $\bullet$ ) cyclobutyl chloride; and ( $\square$ ) allylcarbinyl chloride.

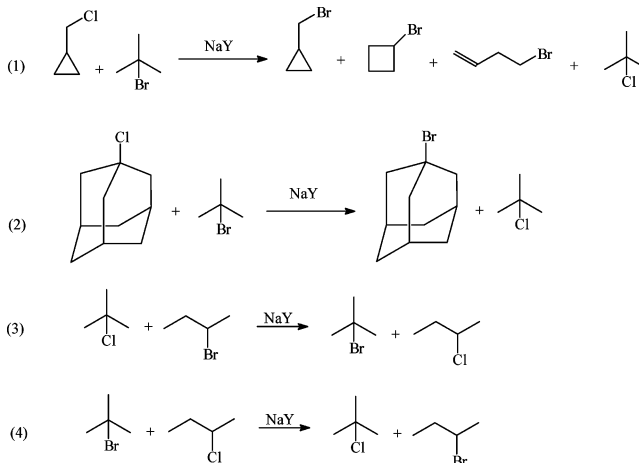
rearrangement of cyclopropylcarbinyl chloride, the ratio of cyclobutyl/allylcarbinyl chloride is 1.0 at 20 min and decreases to 0.1 after 120 min of reaction time, approaching the thermodynamic distribution. In contrast, the same reaction over NaY zeolite results, after 24 h, in a distribution of 0.7 for the cyclobutyl/allylcarbinyl chloride, in spite of the fact that cyclopropylcarbinyl chloride is no longer observed in the reaction medium. In control experiments, we observed that allylcarbinyl chloride is virtually unreactive over NaY at room temperature, whereas Table 1 shows that the cyclobutyl system reacts slower than the cyclopropylcarbinyl, as expected. However, these reactivity patterns cannot completely explain the distribution found on NaY zeolite. It is possible that the attack of the nucleophile on the bicyclobutonium cation does not follow the same pattern as in solution, where the position leading to the allylcarbinyl isomer is less reactive due to electronic effects.<sup>20</sup> The strong interaction of the cation with the zeolite framework and the relative position of the nucleophiles inside the pores might play a role, favoring a distribution not completely governed by the electron density of the cations, but also reflecting the spatial geometry of the cation and of the nucleophile inside the cage. In fact, zeolites have been used to induce asymmetric photochemical reactions,<sup>24</sup> and the metal cations, as well as confinement effects, play a role in the extent of the enantiomeric excess.

**Halogen Switch.** Zeolites are known as solid materials capable of confining and concentrating reactant molecules inside the channels and cages that form their framework structure.<sup>1</sup> We injected an equimolar mixture of cyclopropylcarbinyl chloride and *tert*-butyl bromide in the N<sub>2</sub> stream, and passed it over NaY zeolite at room temperature. Analysis of the products showed the formation of *tert*-butyl chloride as well as cyclopropylcarbinyl, cyclobutyl, and allylcarbinyl bromides, indicating that nucleophilic substitution has occurred on the two substrates. We also observed the same process injecting other alkyl halide pairs. For instance, *tert*-butyl chloride and *sec*-butyl bromide over NaY give rise to formation of *tert*-butyl bromide and *sec*-



**Figure 5.** Representation of the sandwiched carbocations on the zeolite surface.

**Scheme 4.** Halogen Switch Reaction over NaY Zeolite



butyl chloride. These processes have never been reported in solution and might be classified as *halogen switch*. Although the yields do not exceed 3–5%, the observation of halogen switch is another important feature of zeolites as a medium to carry out ionic reactions. In liquid solutions the substrate is completely surrounded by the solvents molecules, impairing the proximity between two different ionogen molecules. Thus, upon ionization, either the solvent or the leaving group (internal return) attacks the formed carbocation. However, on zeolites, the pore structure permits the concentration of two different alkylhalide molecules inside the cavities, allowing the formed carbocations to interact with two different leaving groups (nucleophiles), as pictured in Figure 5. We were also able to observe the halogen switch by initially passing a flow of *tert*-butyl bromide over NaY zeolite and, in the sequence, passing cyclopropylcarbinyl chloride over the same zeolite, observing formation of cyclopropylcarbinyl bromide, cyclobutyl bromide, and allylcarbinyl bromide. Some representative halogen switch reactions observed over NaY are shown in Scheme 4. The fact that 1-chloroadamantane undergoes the reaction is an additional proof for the ionization of alkyl halides inside the zeolite cages. Formation of 1-bromoadamantane was only possible through the nucleophilic attack of the bromide ion on the 1-adamantyl cation. In control experiments, we also observed the same product when reacting 1-chloroadamantane over NaY impregnated with NaBr.

**Theoretical Calculations.** Figure 6 shows the calculated structure of the bicyclobutonium (BCB) and the cyclopropylcarbinyl (CPC) cations, at PBE1PBE/6-31G(d,p):MND0 level, and Table 2 the main geometric parameters, according to the bonding representation shown in Chart 2. We were able to find two minima for the bicyclobutonium cation inside the zeolite Y pore network. In structure BCB (A), two methylene groups are transversal to the T<sub>3</sub> site of the zeolite framework, whereas in BCB (B) the methylene groups are more aligned with the T<sub>3</sub>

(24) Sivaguru, J.; Natarajan, A.; Kaanumalle, L. S.; Shailaja, J.; Uppili, S.; Joy, A.; Ramamurthy, V. *Acc. Chem. Res.* **2003**, *36*, 509.

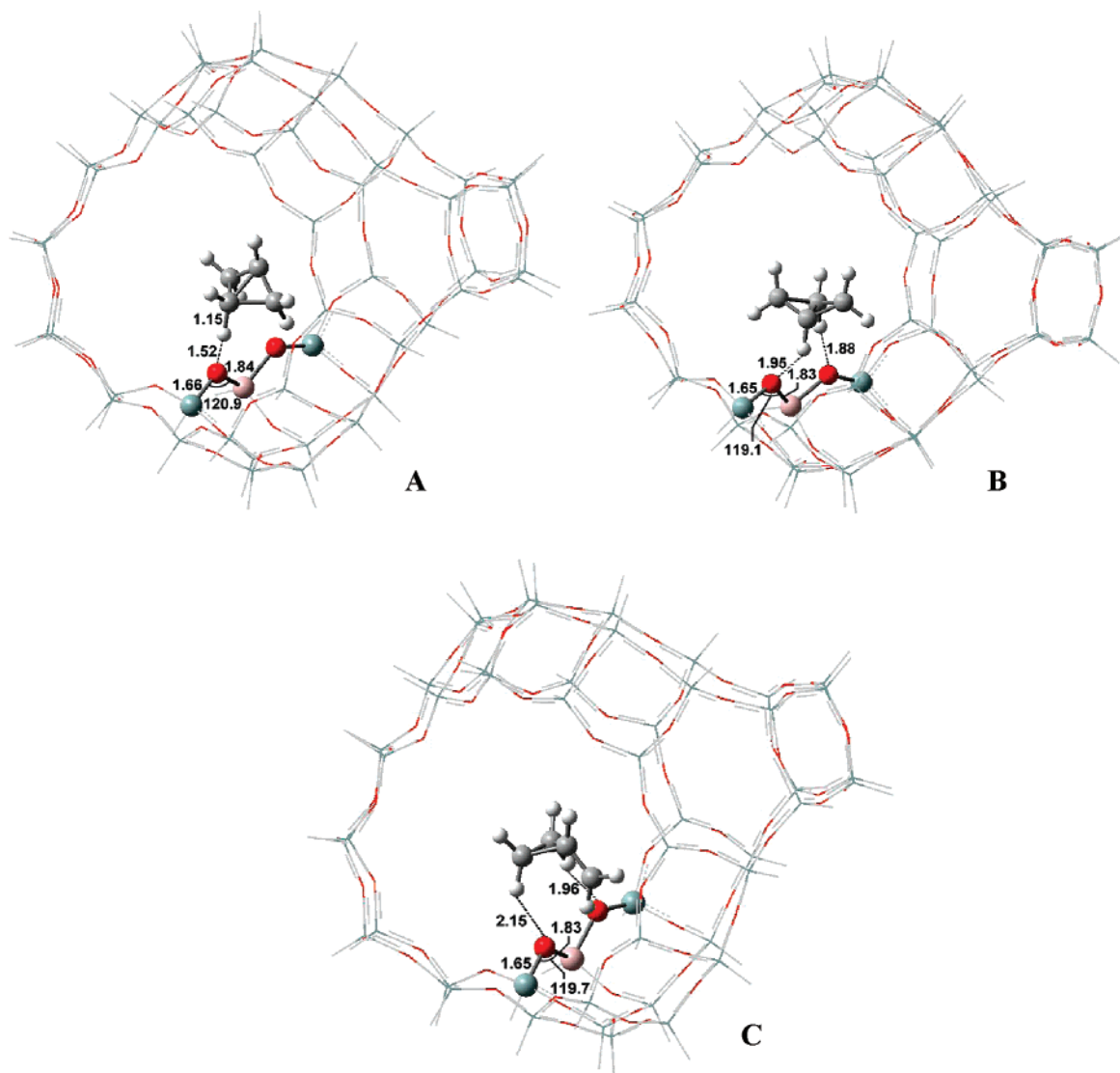


**Figure 6.** Calculated structure of the bicyclobutonium (A and B) and cyclopropylcarbinyl (C) cations inside the zeolite Y cavity, at PBE1PBE/6-31G(d,p):MNDO level.

site. There are minor geometric differences in the structure of the BCB cations, with the exception of the interaction with the zeolite framework. There is a strong hydrogen bond between BCB (A) and the zeolite structure, which is reflected in the O–H bond distance of 1.52 Å, compared with 1.88 Å in BCB (B). The geometric parameters calculated at PBE1PBE/6-31G(d,p):MNDO are very close to the values calculated at MP2/6-31G(d,p):MNDO, indicating that this level of calculation may be used to describe the structure and energy of carbocations inside the zeolite structure, at lower computational costs. There was good agreement among the calculated geometric data for the cations within the zeolite cage and in the gas phase, at similar computational levels. The minor differences may be explained by the interaction of the cation with the zeolite structure.

The strong hydrogen bonding interaction of BCB (A) with the zeolite structure may account for the calculated energy difference of 3.8 kcal/mol, at PBE1PBE/6-31G(d,p):MNDO level, in relation to the CPC cation, as shown in Table 3. The CPC cation is just 0.5 kcal/mol higher in energy than BCB (B) at PBE1PBE/6-31G(d,p):MNDO level. This difference may also be explained in terms of hydrogen-bonding stabilization with the zeolite framework. It was recently reported that *nonclassical*

carbocations may be stabilized by hydrogen bonding.<sup>25</sup> However, the typical hydrogen bond distances in these cases are over 2.0 Å, much longer than the 1.52 Å found for BCB (A). In fact, such a hydrogen bond is only found in some dicarboxylic acids<sup>26</sup> and diamines<sup>27</sup> (proton sponges) and is referred to as a strong or very strong hydrogen bond.<sup>28</sup> The calculations of BCB and CPC cations within the zeolite cages, suggest that carbocations might be stabilized by hydrogen bonding with the framework structure, as similarly suggested for enzymes.<sup>25</sup>

Table 3 also presents the energy differences at other levels of calculation and comparison with the gas-phase energy difference between the two cations. The BCB (A) is lower in energy than the CPC, by 7.8 kcal/mol and 6.5 kcal/mol, at B3LYP/6-31G(d,p):MNDO and MP2/6-31G(d,p):MNDO levels, respectively. However, CPC seems to be slightly more stable than BCB in the gas phase. Casanova et al. reported<sup>20</sup> that in

(25) Bojin, M. D.; Tantillo, D. J. *J. Phys. Chem. A* **2006**, *110*, 4810.

(26) Garcia-Viloca, M.; González-Lafont, A.; Lluch, J. M. *J. Am. Chem. Soc.* **1997**, *119*, 1081.

(27) (a) Staab, H. A.; Staupe, T. *Angew. Chem., Int. Ed.* **1988**, *27*, 865. (b) Alder, R. W. *Chem. Rev.* **1989**, *89*, 1215.

(28) Gilli, P.; Bertolasi, V.; Ferretti, V.; Gilli, G. *J. Am. Chem. Soc.* **1994**, *116*, 909.

**Table 2.** Main Geometric Parameters for the Calculated Bicyclobutonium (BCB) and Cyclopropylcarbanyl (CPC) Cations at Different Levels of Calculations (Carbon Atom Numbering Refers to Chart 2)

| cation/level                  | C <sup>2</sup> H–C <sup>3</sup> H <sub>2</sub> | C <sup>2</sup> H–C <sup>4</sup> H <sub>2</sub> | C <sup>3</sup> H–C <sup>4</sup> H <sub>2</sub> | C <sup>3</sup> H <sub>2</sub> –C <sup>4</sup> H <sub>2</sub> | C <sup>1</sup> H <sub>2</sub> –C <sup>4</sup> H <sub>2</sub> |
|-------------------------------|--|--|--|--|--|
| PBE1PBE/6-31G(d,p):MNDO       |  |  |  |  |  |
| BCB (A)                       | 1.631  | 1.433  | 1.430  | 1.604  | 1.609  |
| BCB (B)                       | 1.643  | 1.418  | 1.427  | 1.661  | 1.624  |
| CPC                           | 1.359  | 1.609  | 1.650  | 1.421  |  |
| B3LYP/6-31G(d,p):MNDO         |  |  |  |  |  |
| BCB (A)                       | 1.662  | 1.436  | 1.433  | 1.621  | 1.634  |
| BCB (B)                       | 1.669  | 1.408  | 1.445  | 1.748  | 1.597  |
| CPC                           | 1.365  | 1.611  | 1.659  | 1.432  |  |
| MP2/6-31G(d,p):MNDO           |  |  |  |  |  |
| BCB (A)                       | 1.627  | 1.432  | 1.430  | 1.605  | 1.608  |
| BCB (B)                       | 1.641  | 1.409  | 1.436  | 1.714  | 1.594  |
| CPC                           | 1.358  | 1.604  | 1.650  | 1.420  |  |
| MP2/6-31G(d) <sup>a</sup>     |  |  |  |  |  |
| BCB                           | 1.650  | 1.425  | 1.425  | 1.649  | 1.649  |
| CPC                           | 1.356  | 1.645  | 1.645  | 1.415  |  |
| B3LYP/6-31G(d,p) <sup>b</sup> |  |  |  |  |  |
| BCB                           | 1.676  | 1.436  | 1.424  | 1.634  | 1.679  |
| CPC                           | 1.359  | 1.639  | 1.679  | 1.420  |  |

<sup>a</sup> Reference 19b. <sup>b</sup> Reference 20.

**Chart 2.** Pictorial Representation of the Bicyclobutonium (BCB) and Cyclopropylcarbanyl (CPC) Structures, Showing the Bonding between the Carbon Atoms**Table 3.** Energy Difference, in kcal/mol, between BCB and CPC at Different Levels of Calculations

| calculation level                            | BCB A | BCB B | CPC |
|--|-------|-------|-----|
| PBE1PBE/6-31G(d,p):MNDO                      | -3.8  | -0.5  | 0   |
| B3LYP/6-31G(d,p):MNDO                        | -7.8  | -2.4  | 0   |
| MP2/6-31G(d,p):MNDO <sup>a</sup>             | -6.5  | -3.0  | 0   |
| MP4/6-311G(d,p)//MP2/6-31G(d,p) <sup>b</sup> |       | 0     | 0   |
| MP4/6-31G(d)//MP2/6-31G(d) <sup>c</sup>      |       | 0.26  | 0   |
| B3LYP/6-31G(d,p) <sup>d</sup>                |       | 2.1   | 0   |
| B3LYP/6-31G(d,p) <sup>d,e</sup>              |       | 0.3   | 0   |

<sup>a</sup> ZPE calculation at PBE1PBE/6-31G(d,p):MNDO. <sup>b</sup> Reference 19a, gas phase. <sup>c</sup> Reference 19b, gas phase. <sup>d</sup> Reference 20, gas phase. <sup>e</sup> Reference 20, including water as solvent.

the vacuum, the CPC cation is lower in energy than BCB by 2.1 kcal/mol, at B3LYP/6-31G(d,p) level. This difference decreases to just 0.3 kcal/mol when a polar protic solvent, like water or methanol, is included in the calculations. This may reinforce the stabilization of the cations through hydrogen bond interactions with the solvent. At the MP4/6-31G(d)//MP2/6-31G(d) level,<sup>19b</sup> CPC is more stable than BCB by 0.26 kcal/mol, whereas both structures presented<sup>19a</sup> the same energy at MP4/6-311G(d,p)//MP2/6-31G(d,p) level, after correction for zero-point energy. In solution, the BCB seems to be slightly more stable than the CPC cation, but they undergo a fast interconversion, which may account for the averaging of the methylene carbons, observed by low-temperature NMR studies.<sup>15</sup> The calculations inside the zeolite pore structure indicate that strong hydrogen bond interactions with the framework contribute to the better stabilization of BCB (A) relative to the CPC cation. Indeed, BCB (A) may be on the potential energy surface for proton elimination to the zeolite framework, as observed by the

long C–H bond distance of 1.15 Å (Figure 6). In contrast, BCB (B) has almost the same energy as the CPC cation, which may account for the similar hydrogen bond stabilization, reflecting the intrinsic stability of the cations.

**Zeolites as Solid Solvents.** The results of cyclopropylcarbanyl and cyclobutyl halide rearrangement and nucleophilic substitution over NaY zeolite may be explained in terms of ionization of the substrate, with formation of bicyclobutonium or cyclopropylcarbanyl cation. Nevertheless, one may argue what is the role of the zeolite structure in ionizing the halide.

The polarity of the zeolite Y environment has been compared with the polarity of methanol–water solutions.<sup>29</sup> However, metal-exchanged zeolites are not normally used as catalysts, due to their weak acidity, mostly of Lewis type. A recent study on the photochemical ionization of 2-chloro-1-(4-methoxyphenyl)ethyl acetate showed a positive variation in the activation entropy ( $\Delta S^\ddagger$ ), whereas the same reaction in aqueous solution presents a negative variation.<sup>30</sup> These results were interpreted in terms of the rigid zeolite Y structure not interfering much in the ionization process, especially in terms of steric repulsions to assist the solvation of the transition state. In solution, the solvent molecules reorganize themselves to accommodate the electronic and geometrical changes when the reaction proceeds to the transition state.<sup>31</sup> Such a new reorientation is not possible in zeolites, as the structure is somewhat rigid, impairing long-range deformations.

The confinement effects of zeolites have long been recognized in the literature.<sup>32</sup> This property has been explored by Derouane, to propose that zeolites act as solid solvents,<sup>33</sup> in terms of partition coefficient of reactants inside and outside the pore system. Another important property of solvents<sup>34</sup> is their ionizing ability, with the presence of electron-pair donor (EPD) and electron-pair acceptor (EPA) sites in the structure. For instance, in water, the EPD interactions occur through complexation of the cationic part of the ionogen substrate with the lone electron pairs of the oxygen atom, whereas the EPA interactions take place through hydrogen bonding with the anionic ionogen moiety in the transition state. Many organic liquids, as well as molten salts or ionic liquids<sup>35</sup> also possess EPA–EPD centers, and act as solvents. We may also interpret that the oxygen atoms of the framework structure of zeolite Y act as EPD centers, whereas the sodium metal cations act as EPA centers. Thus, we may consider NaY as a solid solvent, not only in terms of partition coefficient, but also as a medium to ionize alkyl halides.

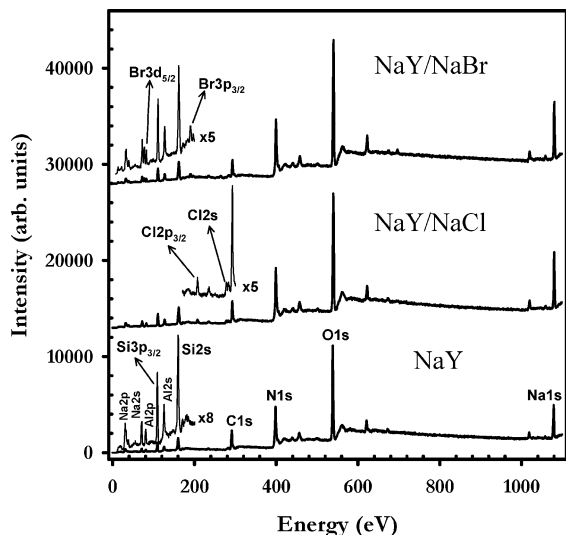
We showed that nucleophilic substitution reactions do occur when NaCl or NaBr are impregnated on the NaY zeolite. To have further insights of the dispersion of the sodium halides into the zeolite channels, we carried out XPS measurements of the parent and impregnated zeolites. This technique permits a semiquantitative analysis of the external surface of the zeolite, helping to characterize the dispersion of the sodium halides

- (29) Ortiz, W.; Cozens, F. L.; Schepp, N. P. *Org. Lett.* **1999**, *1*, 531.  
 (30) Schepp, N. P.; Monk, W.; Cozens, F. L. *J. Am. Chem. Soc.* **2004**, *126*, 1012.  
 (31) Winstein, S.; Fainberg, A. H. *J. Am. Chem. Soc.* **1957**, *79*, 5937.  
 (32) (a) Rabo, J. A.; Bezman, R. D.; Poutsma, M. L. *Acta Phys. Chem.* **1978**, *24*, 29. (b) Derouane, E. G. *J. Catal.* **1986**, *100*, 541.  
 (33) (a) Derouane, E. G. *J. Molec. Catal. A* **1998**, *134*, 29. (b) Derouane, E. G.; Crehan, G.; Dilom, C. J.; Bethell, D.; He, H.; Abd-Hamid, S. B. D. *J. Catal.* **2000**, *194*, 410.  
 (34) Reichardt, C. *Solvent and Solvent Effects in Organic Chemistry*; VCH-Verlag: Weinheim, 1988.  
 (35) Dupont, J.; de Souza, R. F.; Suarez, P. A. Z. *Chem. Rev.* **2002**, *102*, 3667.

**Table 4.** Atomic Ratios of Parent and Impregnated NaY Zeolites Obtained by XPS Analysis

| zeolite  | Si/Al <sup>a</sup> | Si/Na | Si/X <sup>a,b</sup> (XPS) | Si/X <sup>c</sup> (nominal) |
|----------|--------------------|-------|---------------------------|-----------------------------|
| NaY      | 2.2                | 1.9   |                           |                             |
| NaY/NaCl | 1.9                | 1.3   | 6.2                       | 5                           |
| NaY/NaBr | 1.9                | 1.2   | 6.2                       | 5                           |

<sup>a</sup> Areas from Si(1s), Al(1s), Na(1s). <sup>b</sup> Areas from Cl(2p) and Br(2p). <sup>c</sup> Obtained by chemical analysis.

**Figure 7.** XPS spectra of the parent NaY and NaY impregnated with NaCl and NaBr.

inside the pores. The results are shown in Table 4 and Figure 7. The atomic Si/Al ratios of the parent and impregnated zeolites are close to the nominal ratio, obtained by chemical analysis, showing that the silicon and aluminum atoms are well distributed along the zeolite crystal. The atomic Si/Cl and Si/Br ratios obtained by XPS analysis show that impregnation led to a well-dispersed material, probably forming ion pair nanoparticles of sodium halide inside the zeolite cavities. The atomic Si/X ratio ( $X = \text{Cl}, \text{Br}$ ) at the external surface is slightly higher than the nominal ratio, based on chemical analysis, indicating that the halides moved inside the zeolite channels. This may allow the nucleophilic attack of the bromide or chloride anions to the formed carbocation. A similar situation was observed<sup>36</sup> for KSCN over  $\text{Al}_2\text{O}_3$ , which presented a band at  $2075\text{ cm}^{-1}$ , together with the asymmetric  $\text{SCN}^-$  stretching at  $2050\text{ cm}^{-1}$ . The former band was associated to a well-dispersed KSCN phase on the alumina surface and is dependent upon the loading. This material showed increased reactivity as a reagent for the synthesis of tert-alkyl thiocyanates. It should be also mentioned that ionic conduction in sodalite and cancrinite is enhanced<sup>37</sup> by the introduction of halide anions, supporting our XPS results that show a well-dispersed impregnated zeolite. In the XPS spectra of Figure 7, we were able to observe the presence of carbon and nitrogen species at the external zeolite surface, although the chemical analysis did not detect significant amounts of these elements. The peaks were present in the parent and impregnated zeolites, indicating that they were already present in the starting material, probably as external impurities during

NaY synthesis. In fact, it has already been reported<sup>38</sup> that carbonate species, probably formed upon the interaction with atmospheric  $\text{CO}_2$ , might be present at the external surface of oxide material and observed by XPS measurements. In addition, the sticky tape used to introduce the samples in the chamber might also contribute to these peaks.

It has already been reported that zeolite Y can be used as a host for growing<sup>39</sup> zinc oxide nanoparticles, with sizes as small as 1 nm, upon impregnation and calcination of zinc nitrate. We report here that NaCl and NaBr impregnated Y zeolite may be used as a medium to carry out nucleophilic substitution reactions, implying that zeolites act as solid solvents, dispersing ionic reactants such as inorganic salts inside the cavity. This approach may be further explored in other reactions, where polar protic solvents, like water, cannot be used.

Finally, one may ask, why NaY zeolite cannot be just considered a Lewis acid catalyst, similarly to  $\text{FeCl}_3$  or  $\text{ZnCl}_2$ ? In fact, the behavior of an EPA center is similar to that of a Lewis acid. Nevertheless, a Lewis acid–base interaction involves the formation of bonds with considerable more covalent character than EPA–EPD association. Thus, although we recognize that the sodium cation act as EPA centers in NaY zeolite, we do not interpret this behavior as strictly in terms of Lewis acidity. We have shown that ion–dipole interactions govern<sup>13a</sup> the EPA–EPD association of the sodium cation with the halogen atom of the alkyl halide, not causing great geometric changes, consistent with the behavior of a solvent and not a Lewis acid catalyst. In addition, the ability to disperse the sodium halide particles is typical of a solvent, rather than a Lewis acid.

## Conclusions

It was shown that rearrangement and nucleophilic substitution of cyclopropylcarbonyl and cyclobutyl halides occurs on NaY zeolite impregnated with sodium halide. The rate of cyclopropylcarbonyl bromide rearrangement was not significantly affected by whether or not the NaY zeolite had been impregnated with NaCl, suggesting a first-order process, with ionization to bicyclobutonium or methylcyclopropyl carbocations. The distribution of the alkyl chlorides formed is neither that found in nucleophilic solvolysis, nor the thermodynamic ratio, which would give more than 99% of the allylcarbonyl chloride.

We report a new process of nucleophilic substitution, namely “halogen switch”, involving alkyl chlorides and bromides of different structures, switching the halogen atoms between the substrates. This reaction occurs inside the pores of the zeolite, due to confinement, which localizes the carbocation between two different nucleophiles.

Calculations showed that the bicyclobutonium (BCB) and cyclopropylcarbonyl (CPC) cations might be intermediates within the zeolite cages. The BCB cation is thermodynamically more stable, due to strong hydrogen bond interactions with the zeolite framework. The calculations, together with the experimental results of nucleophilic substitution and halogen switch, are strong evidence for the formation of carbocations as intermediates within the zeolites pores. We might also infer that there

(36) Ando, T.; Clark, J. H.; Cork, D. G.; Fujita, M.; Kimura, T. *J. Org. Chem.* **1987**, *52*, 681.

(37) Jordan, E.; Bell, R. G.; Wilmer, D.; Koller, H. *J. Am. Chem. Soc.* **2006**, *128*, 558.

(38) Barr, T. L.; Chen, L. M.; Mohsenian, M.; Lishka, M. A. *J. Am. Chem. Soc.* **1988**, *110*, 7962.

(39) (a) Wark, M.; Kessler, H.; Schlz-Ekloff, G. *Microporous Mater.* **1997**, *8*, 241. (b) Bouvy, C.; Marine, W.; Sporken, R.; Su, B. L. *Colloids Surf. A: Physicochem. Eng. Aspects* **2007**, *300*, 145.



exists an equilibrium between the carbocations and the respective alkoxides.

Zeolites might be considered solid solvents, providing a medium to favor ionization and disperse nucleophilic species. The XPS measurements of NaY impregnated with NaCl and NaBr indicated that sodium halides are well dispersed inside the cavities, as shown by the Si/X atomic ratio.

**Acknowledgment.** The authors thank CAPES, CNPq, and FAPERJ for financial support. They also acknowledge the LNLS (Research Proposal D04A-SXS-5725) for the XPS characteriza-

tion of the zeolites. The authors also thank Mr. Mauri Cardoso from CENPES/PETROBRAS for helpful discussions concerning the XPS spectra of the impregnated zeolites.

**Supporting Information Available:** Complete reference 22 and tables with the Cartesian coordinates, total energy, ZPE and thermal corrections of the calculated carbocation/zeolite systems. This material is available free of charge via the Internet at <http://pubs.acs.org>.

JA0742939